Ric Zhang

DE2: Gizmo

Contents

1) Abstract

The reduction of size in electronic components and batteries has paved the way for the creation of a new generation of robots. Smaller and more efficient, these new robots have a wide variety of sectors and tasks that they could operate in such as quick and low-risk scouts in a search and rescue situation to laying down power lines in small locations that humans are not able to enter.

Although un-conventional, using jumping (or rather saltatorial locomotion) as a primary form of movement would create multiple benefits. In nature, saltatorial movement provides sudden bursts of speed to allow larger obstacles to be overcome and prey to be caught. Continuous jumps with a constant frequency have also been proved to be a very efficient form of moving at high speeds [1].

2) Introduction

2.1) Project Brief

The given project brief specifies for a monopod jumping robot to be designed and modelled with CAD and then specified with further general assembly and part drawings. Technical specifications to be met are set out in table 1. Additional requirements include the ability to self-right after a jump as well as the optional inclusion of a steering mechanism for in-flight control.

Criteria	**Requirements**
Jump height	300 mm
Range	300 mm
Mass	100 g to 200 g
Cost	Under 100 GBP
IP rating	IP54

Table 1: Technical Specifications of Build

2.2) Executive Summary

Design led to a robot that, in theory, would be able to meet the requirements for jump height and distance, weight, cost, ingress protection but is unable to self-right after a jump. A research stage involving biomimetics and an extensive amount of calculations was used to design initial sub-assemblies with components that would allow the robot to perform as intended. Further improvements need to be made to allow for in-flight control and self-righting.

3) Synthesis

3.1) Research

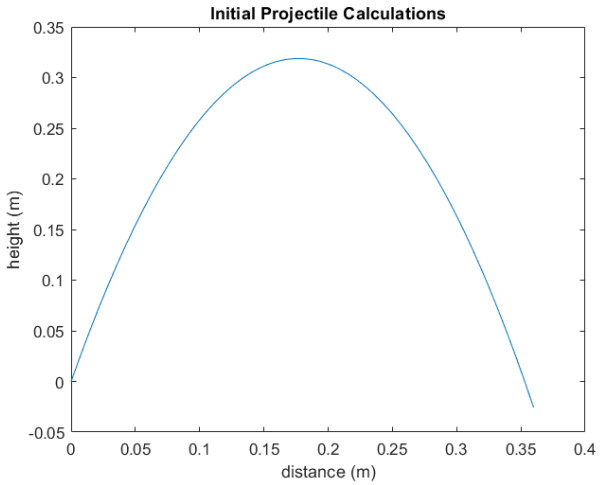

Figure 1: Initial Projectile Plot

```
%---------------Drag_Calulation-----------------------
CD = 1.2; % drag coefficient
Ar = 0.0036; %contact area (m^2)
Mass = 0.2; %(kg)
v = 2.7; % inital launch speed (m/s)
theta = 75; % degrees to the horizontal

ro = 1.225; % density of jump medium (kg/m^3)
g = 9.81; % gravitational constant
c = (0.5*ro*CD*Ar)/Mass; % drag force calculation
```

Figure 2: Projectile Calculation Variables

To understand the performance requirements for different components, calculations regarding the projectile motion of the robot in flight needed to be made. Modelling the path of a jump requires a second order differential equation which was achieved with MATLAB.

A numerical solver for projectile motion was made and worst-case conditions were used (as seen in Figure 2). Launch speed and launch angle were varied until an optimum solution was found which requires an initial speed of 2.7 ms^{-1} at 75 degrees to the horizontal.

A simple energy calculation shows that each jump requires 0.729 joules. Assuming that the transmission system between the stored energy and output is 50% efficient means that 1.458 joules of energy will be required to be stored per jump.

K.E=1/2 mv^2

$$\frac{1}{2} \times 0.2 \times 2.7^2$$

$$= 0.729$$

To understand the amount of power the robot will require for a jump the amount of time between the moment from the start of a jump to when the foot leaves the floor is required. The amount time for this action to take place is un-intuitive to estimate. To determine a correct value for jump time, data was created by analysing footage of SALTO, a grasshopper and a kangaroo rat with Tracker 5.0; a free software that can analyse footage and track a point to plot its speed and position (use of Tracker is shown in figure 3). Results of the three studies are shown in table 2.

Test Subject	**Jump time (s)**
Grass-hopper	0.025
Kangaroo Rat	0.042
SALTO	0.064

Table 2: Jump Times of Various Subjects

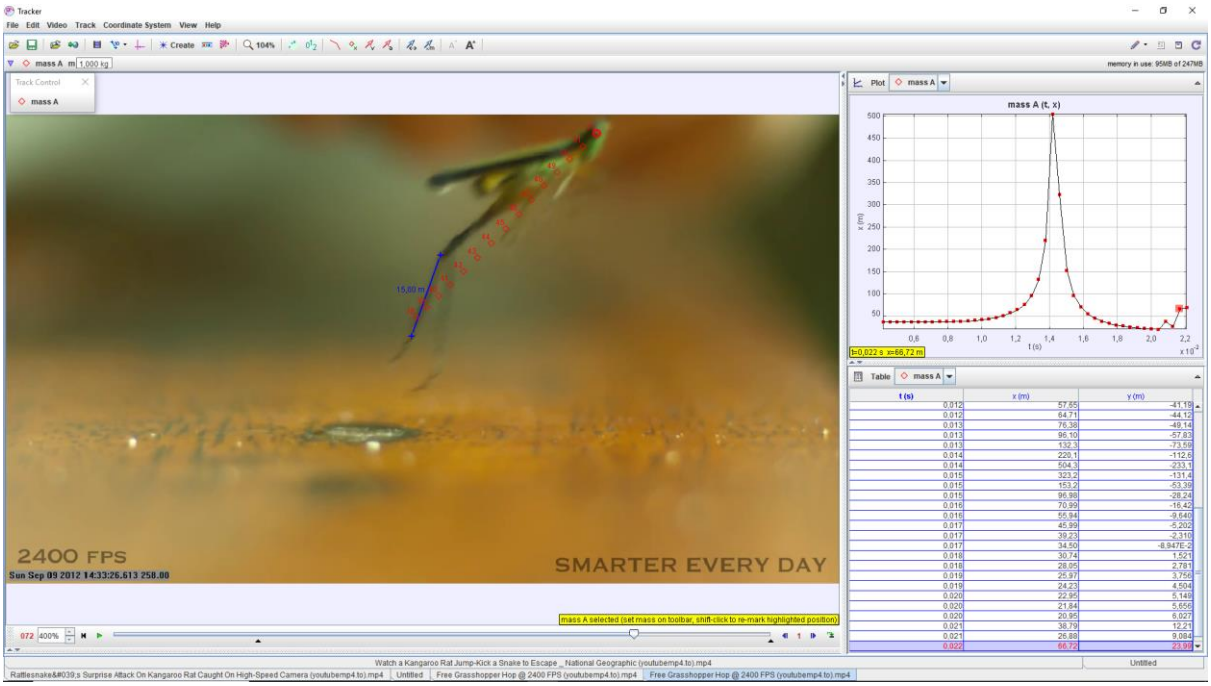

Figure 3: Jump Time Calculations with Tracker

Results consistently show times jump times in the magnitude of tens of microseconds. By analogy we can assume that any robot designed in this scale of size will have a similar jump time. If this deduction is true, the power supplied for the jump will need to be roughly 30 Watts (1.46/0.05). This is an un-realistic amount of power to supplied by a motor that would fit the brief in terms of weight, size and cost; an intermediate form of energy storage is required to suddenly supply this amount of power, the simplest way to achieve this would be implementing a spring.

Alternative options such as releasing energy from compressed gas or a small explosive were explored but rejected after deciding that both methods would create too much randomness during a jump. Batteries have the benefit of being widely available and easily replaced or re-charged so the robot could be continuously re-used in isolated conditions.

3.2) Biomimicry

Biomimicry has always existed in the world of engineering and possibly been most prevalent in the sector of robotics. Nature has had the ability to iterate and refine designs over the course of millions of years through evolution, we still struggle to come close to achieving the same level of performance seen in animals. While copying the behaviours, mechanisms and materials found in nature offers an accelerated path to design, it should be noted that there are properties that can't achieved when using biomimicry. Most notably, mechanical efficiency is much more difficult to improve upon. It is estimated that animal joints have coefficient of friction as low as 0.003 [2].

Figure 4: A Peacock Mantis Shrimp

Although similar coefficients can be reached with bearings, this can add considerable amounts of weight and cost to a build.

It should be noted that in animals, strength and volume are not linearly proportional to each-other. As a simple explanation, this is due to the fact that the power of muscle is proportional to the cross-sectional area of muscle (roughly proportional to length squared) while volume is proportional to length cubed. This is relevant when looking for creatures to mimic, scaling pre-existing mechanisms such as that of a flea to achieve the requirements of the brief will result in failure.

In the search for a mechanism to suddenly release a large amount of kinetic energy, the mantis shrimp was observed. The shrimp stuns and kills its prey with its claws, which travel at 23 ms^{-1} after going through accelerations of 104 kms^{-2} [3]. It achieves this with a speed-amplifying four bar linkage and a specialised saddle-shaped spring made of shell which stores elastic energy. This mechanism is primed by contracting muscles and elastic is energy is stored and released with a latch inside the claw.

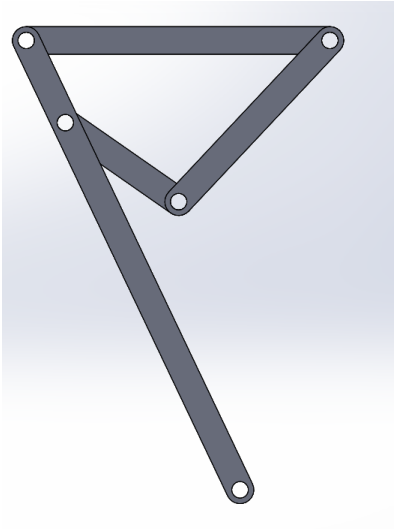

Figure 5: Initial Leg Design

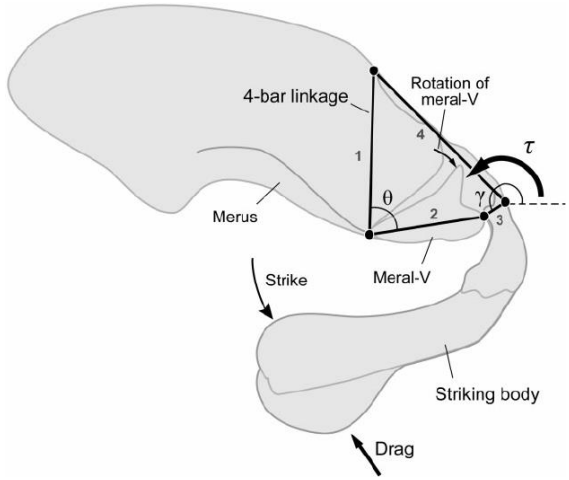

Figure 6: 4 bar Diagram of a Mantis Shrimp Arm

The design of the mantis shrimp's claw mechanism was taken as a base design for the leg linkage mechanism in the robot. Later in design it was discovered that it is possible to double up the speed amplification created by the bar linkage by turning the output of one four bar linkage into the input of another similar linkage.

3.3) Calculations

Spring Selection

A conservation of energy equation can be used to find the total spring constant required. This method initially assumes that the final kinetic energy of the robot is equivalent to the initial elastic energy stored inside of the spring. It was assumed that the deflection of the spring would be 90° as this seemed to be an achievable target during design.

$$\frac{1}{2}mv^2 = \frac{1}{2}k\theta^2$$

$$\frac{1}{2} \times 0.2 \times 2.7^2 = \frac{1}{2} \times k \times \left(\frac{\pi}{2}\right)^2$$

$$k = 0.2 \times \frac{2.7^2}{\left(\frac{\pi}{2}\right)^2}$$

= 0.59 Nm rad^{-1}

Assuming 50% efficiency

1.18 Nm rad^{-1}

Figure 6: Spring Property Calculations

In a final step to account for losses through inefficiencies in linkages, the required spring constant is doubled. The required spring constant of a complete torsion spring system is 1.18 Nm rad^{-1} (equivalent to 7.41 Nm per turn). At full compression, this spring would exert a torque of 1.85 Nm.

Jump Time

By knowing the distance travelled during the extension of a jump while the robot's foot is still in contact with the floor and the jump velocity it is possible to calculate the duration of a jump. This was performed to compare against previous values found from Tracker analysis to ensure a realistic set of values have been calculated and methods for finding critical values for mechanical properties such as the spring constant and energy of a jump were correct.

This check was performed after rough designs for a leg linkage had been made; comparing lengths at contracted and fully extended states shows a total extension of 65 mm. Equations and calculations are shown in figure 7 and provide a result of 48 milliseconds which is in the same order of magnitude as other similarly sized jumping robots and animals. From this it can be inferred that previous calculations have been correct although there still may be some variations in true values due to un-accounted for inefficiencies.

$$t = \frac{S}{\frac{V_f - V_i}{2}}$$

$$t = \frac{0.065}{\frac{2.7 - 0}{2}} = 0.048$$

Figure 7: Jump Time Calculations

3.4) Development

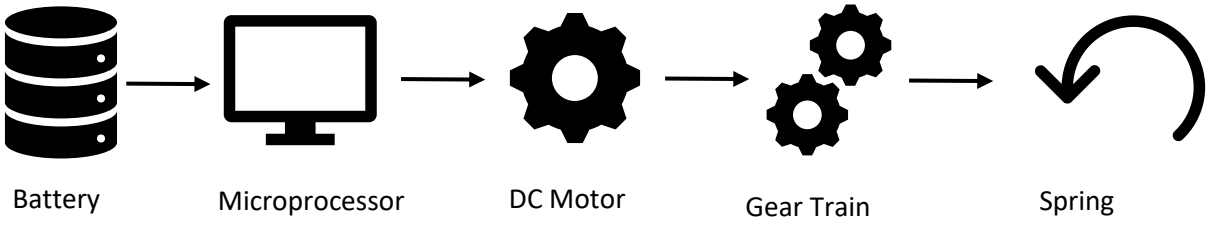

Figure 8: Rudimentary Systems Block Diagram

The above rudimentary block diagram shows the initial plan for systems to be arranged inside of the robot. All components are linked together and therefore their requirements are dependant on each-other and thus parts had to be selected at the same time to ensure that they all worked together while staying under limitations for power, cost and weight. This selection process started at spring design where a custom spring was created with detailed calculations (which are conveyed in detail in section 4.3). A motor was selected for its high torque while being low in cost and weight.

Component	Manufacturer	Price
Battery	Crazepony	£10.99
Motor	Canon	£23
Gear Train	Trident	£58.00
Spring	Self-Made	£0.50

Table 3: Bought Component List

Batteries were selected next to meet the requirements of the motor while contributing to cost and weight minimally. Initially there was difficulty in finding a battery with a large capacity to provide several jumps but a low weight to allow for more freedom during the design of the rest of the robot. The novel approach of connecting 3 small drone batteries which were rated at 3.7 V for a total of 11.1 V was used. In total the set of batteries weighs 16.2 g, an order of magnitude below alternatives that had been found.

By knowing the maximum of torque of the selected motor and compressed spring, calculations could then be done to find the gear ratio required to fully wind the spring (maximum torque of compressed spring over maximum suppliable torque from motor). This was found to be 1:816 which could be achieved with Trident's GS38.900. The component additionally has a relatively low weight and size for its ratio. Final selected components are shown in Figure 9 and prices (totalling to £92.49) are noted in table 3.

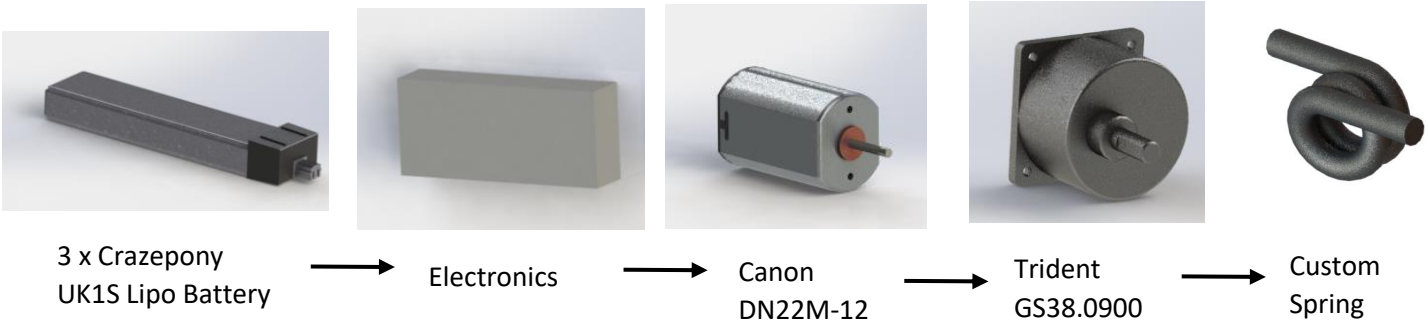

Figure 9: Final Systems Block Diagram

3.5) Material Selection

The constraint of a maximum weight of 200 g severely limited the available materials throughout the build. Wall thickness has been reduced and denser materials such as steel are only used in locations where the higher material properties are justified. In the legs carbon fibre was selected for its high strength to weight ratio, the tubes that are specified in the CAD model are also readily available to buy. The majority of the body which contains housing and other non-moving parts have been constructed from ABS. Relevant beneficial material properties of ABS include high impact resistance, low density, low cost and being impermeable to water.

3.6) Manufacturing

The majority of components are made from ABS, while consideration has been taken to create simple geometries that could be traditionally moulded, there are bespoke parts that have forms that are either difficult to machine by hand or un-formable in one piece. On a small scale of manufacture, these irregular geometries are less of a complication as the use of 3D STL printing could be used to create parts. STL printing is an additive manufacturing process that uses UV light to cure a resin layer by layer. This results in a higher surface resolution and better mechanical properties when compared to traditional FDM printers. Additionally, surfaces can be easily printed to be water-tight and joined with any waterproof epoxy of adhesive for plastics. Part of the robot's design relies on the use of sealants and adhesives to join components and make certain enclosures water-tight. During assembly, these connections could be made with a guide or jig to align pieces as adhesives harden. Other connections involve simple manual labour such as threading bolts at joints and fixing legs to joints with tight interference fits.

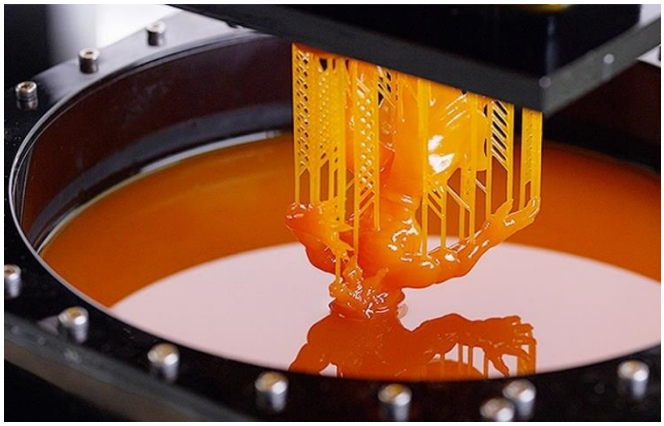

Figure 10: SLA 3D Printing

3.7) Testing

When designing for ingress protection, a product will only be validated after it has been thoroughly. Figure 11 shows a product being tested for its liquid ingress protection, it will be sprayed by jets of water for an extended time from as many angles as possible.

Figure 11: IPX4 Test Rig

To design to meet these criteria, a single enclosure has been made where water-sensitive components are grouped, this reduces points of failure. Sealants can be used to protect joints from allowing water in. At the singular interface where the casing must be opened to allow batteries to be replaced, a rubber gasket has been made to act as a seal after the casing and lid have been fully joined by a set of three M2x6mm bolts.

4) Engineering Analysis

4.1) Failure Analysis

Component design relied on the analysis of forces that would be exerted during a jump. Initially, there are areas of potential failure than can be validated to be safe with one quick calculation. Examples include the maximum torque of the gearbox (of 2 Nm) not being exceeded and checking the true output torque of the DC motor due to the under-volting caused by using 3 3.7 V batteries in series. Components which experienced higher forces and thus had a higher probability of failure were analysed in more detail to ensure successful operation. The highest stresses in the build are located at components in contact with the torsion spring as it is being wound.

The “winder” experiences large torsional forces as one side of it is being turned by its gear and the other is subjected to the full force of the fully wound spring. This creates a torque and applied bending moment of 1.85 Nm each.

$$n = \frac{S_y}{\frac{32}{\pi D^3}\sqrt{M^2 + T^2}} \quad \left| \quad \frac{350 \times 10^6}{\frac{32}{\pi \times 0.005^3} \times \sqrt{1.86^2 + 1.86^2}} \right.$$

$$= 1.63$$

Figure 12: Safety Factor of an Axel Calculations

The above equation defines the safety factor for a shaft with relevant parameters and values. Inserting the tensile yield strength of steel and a diameter of 5mm into the equation returns a safety factor of 1.63.

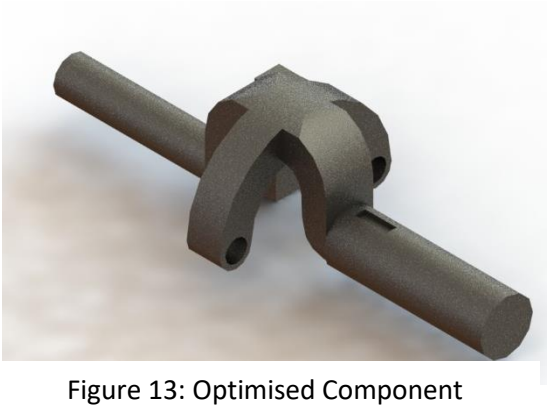

Figure 13: Optimised Component

As the torsional load is distributed between the point of contacts of the spring and gear along the winder, it is assumed that the diameter of rod outside of this region can be reduced.

It is most likely that fatigue will be the cause of failure in this component. The design of the release mechanism means that the maximum force of the torsion spring will always be the same and it is unlikely that the component will every experience an abnormally high load. The component will however experience the same load in the same direction for its entire life of use. To extend the life of the component of thus mitigate chance of failure, the shaft has the relatively high safety factor of 1.63.

The Lewis Factor equation can be used in engineering to select the minimum tooth width of a gear. It is dependant upon the torque and angular speed at the input as well as the modulus, Lewis form factor, pressure angle, number of teeth and tensile strength of the gear’s material. Clearly there are

many factors that can be changed to alter the required face width, one of them being the method of production for said gear. Precision formed gears formed generally allow for smaller tooth widths.

$$P = \tau \times \omega$$

$$F_t = P/V$$

$$V = d \times \omega$$

$$K_V = \frac{6.1 + V}{6.1}$$

$$b_a = \frac{K_V \times F_t}{\sigma \times m \times Y}$$

$$\frac{2.29 \times 17}{77 \times 1 \times 0.28} = 1.8$$

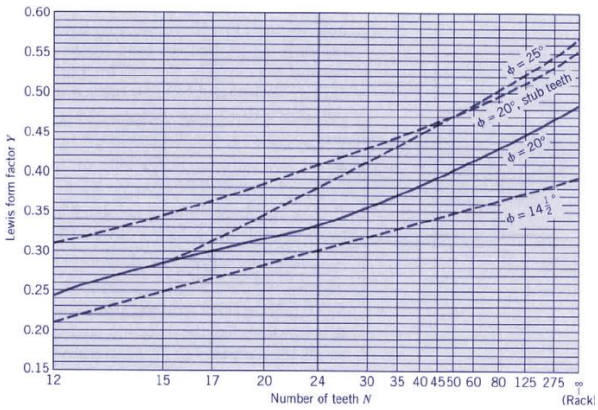

Figure 14: Lewis Factor Calculations

The working in figure is relevant to the first gear of the gear train, attached directly to the output rod of the Canon DNNM-12. After calculating values for the various constants and assuming that the gear will be formed by milling, the minimum tooth width is 1.8 mm. The actual tooth width in the design is 3mm which means that there is a safety factor of 1.7 in this gear. Again, fatigue is the most likely form of failure for gears due to their constant cyclic stresses. In an effort to reduce the possibility of focusing forces on one specific tooth repeatedly which would result in a quicker fatigue, gear ratios are selected to not be a whole number. This means that the same teeth will not mate with each other every time and thus distribute forces more evenly across the teeth of the gear.

Figure 15: Optimised Gear

Across the rest of the robot the most likely modes of failure include impact, particularly in the thin casing and brittle carbon fibre legs, due to the randomness of possible landing orientations, the main way to mitigate these forms of failure is to increase the safety factor of parts. These improvements would mostly consist of adding extra material to spread stresses more. This has been attempted although improvements are minimal as the weight limit had been exceeded in the first iteration of design.

4.3) Spring Design

A custom spring was required to be made to meet the requirements for the build efficiently, the equation in figure 16 was used for this. From previous calculations it was known that the spring constant of the designed spring would have to be above 7.41 Nm per turn. Various configurations of wire diameter, spring diameter and number of turns were tested until the current values seen in Figure 16 were used to achieve a spring with the required spring constant and size that would fit into the robot design at the time.

$$k = \frac{d^4 E}{10.2DN} \qquad \frac{79.3 \times 1.76^4}{10.2 \times 5 \times 2} = 7.46$$

Figure 16: Spring Dimension Calculations

Additionally, it had to be ensured that the diameter of the spring was greater than the minimum spring diameter at full deflection. The modelled spring in Solidworks accurately follows set parameters and has an inner diameter of 3.24 mm, this is greater than the calculated minimum inner diameter or 2.68 mm and thus in theory the spring should work. Calculations are shown below.

$$D_{i\ min} = \frac{DN_b}{N_b + \theta'} - d \qquad \frac{5 \times 2}{2 + \frac{1}{4}} - 1.76 = 2.68$$

Figure 17: Minimum Inside Spring Diameter Calculations

5) Final Design

5.1) Designed Components

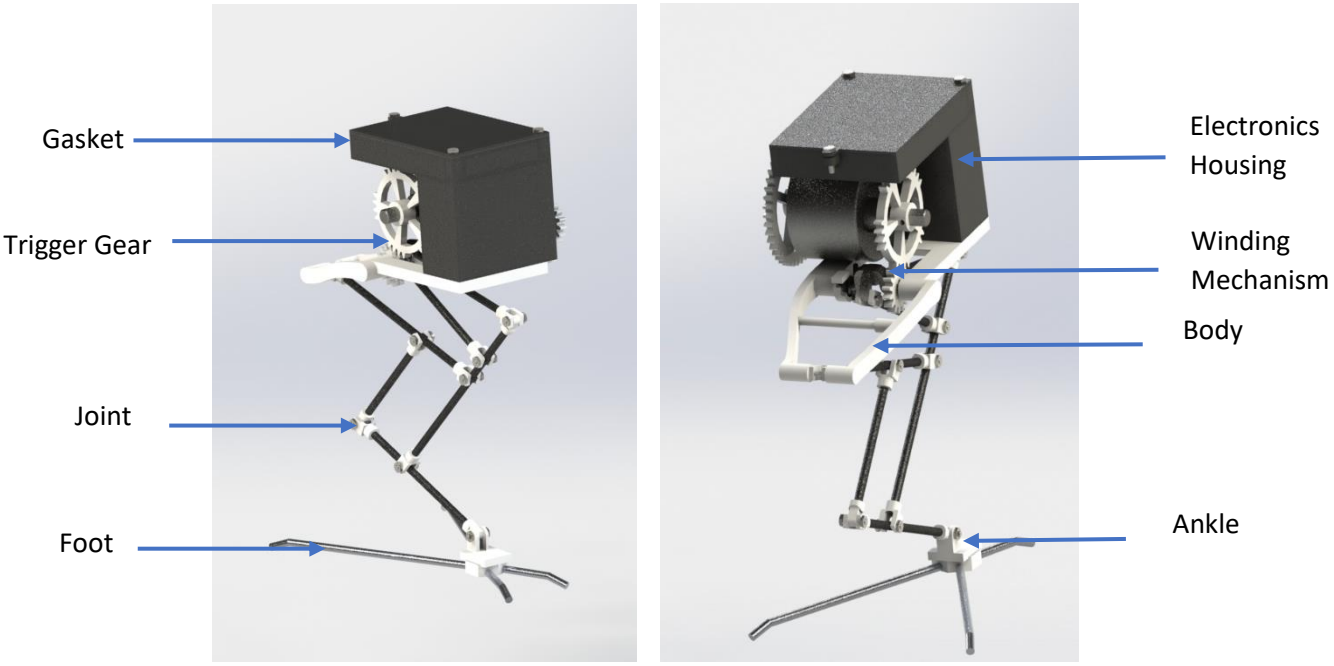

Figure 17: Specially Engineered Components

The final design for the robot has multiple specialist components that are created for specific purposes. These bespoke components have been highlighted in figure 17, some of these components are elaborated upon in the following section.

The winder component (see figure 13) is designed to increase the allowed deflection of the spring as it removes material that begins to foul and prevent movement at deflections greater than 70° . Although the component is difficult to machine, it increases the performance of the robot and is deemed a necessary component.

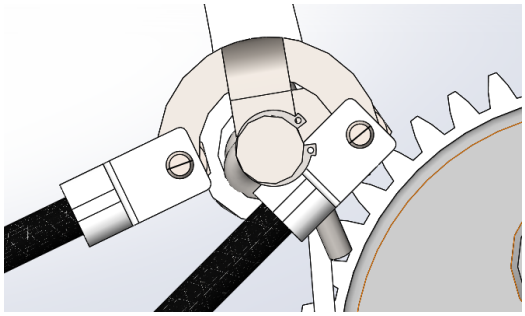

Figure 18: Clearance Created by Specialised Component

The Gear trigger is designed to be act as a simple trigger mechanism for the primed spring. It works by having sets of four teeth followed by a gap of 3-teeth on a 35-tooth gear. The four teeth are enough to wind the gear back a quarter turn and provide the stored elastic energy for a jump. After the fourth tooth has left the full gear that is connected to the wound spring has no mate. This will allow the wound gear to freely spin in the gap of 3 teeth as the spring returns to a deflection of 0° . The stresses found on the gear teeth should be no different to normal as in normal cases, spur gears only mate at one tooth at a time.

Figure 19: Trigger Gear

Additional modification compared to a standard gear include the removal of material from the flat of the gear; this was done to meet weight requirements set in the brief and decreases the mechanical properties of the gear. However, it is assumed that this is a reasonable decision as the main point of failure for the gear is in the teeth and increased stress within the body of the gear will have little effect on the chance of failure under normal load conditions.

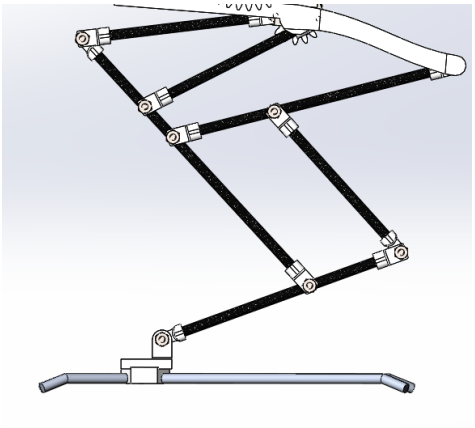

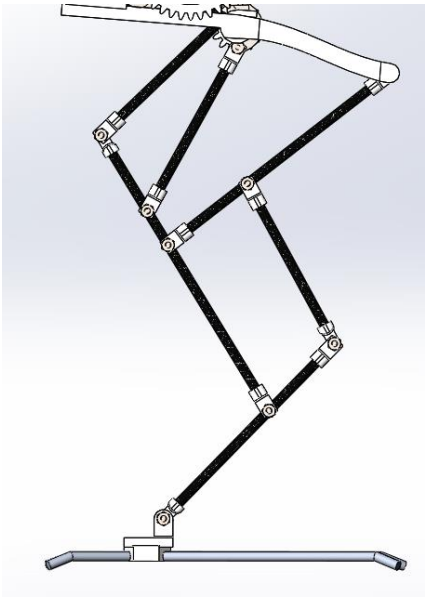

Figure 20: Compressed and Extended 8-Bar Leg Linkage

The 8-bar linkage that is used for the leg has multiple purposes. As previously stated the mechanism is derived from a mantis shrimp's arm and serves as a tool to amplify speed. It also provides the 75° launch angle required to achieve a horizontal distance of 30 cm. This is achieved by the output of the mechanism, which is connected to the foot, moving on a line that 25° to the horizontal of the centre of mass of the robot.

5.2) Conclusion

Although much analysis has been done, a physical model of the design would be required to test if the robot can operate as expected. Additional improvements in component selection would possibly allow for the self-righting criterion to be met.

6) References

1) Conger, C. 'Why Do Kangaroos Hop?' . 5 August 2008 . retrieved from https://animals.howstuffworks.com/mammals/kangaroo-hopping1.htm

2) Qiu, C. 'Coefficients Of Friction Of Human Joints'. 2007. Retrieved from https://hypertextbook.com/facts/2007/ConnieQiu.shtml

3) Pateck, S.N, 'Deadly stricke Mechanism of a Mantis Shrmp'. 22 April 2004. Retrieved from https://pateklab.biology.duke.edu/sites/pateklab.biology.duke.edu/files/Pateketal2004Nature.pdf

ITEM NO.	PART NAME	MATERIAL	QTY.
1	50mm Leg	CARBON FIBRE	3
2	85mm Leg	CARBON FIBRE	1
3	90mm Leg	CARBON FIBRE	1
4	70mm Leg	CARBON FIBRE	1
5	Female Joint	ABS	9
6	Male Joint	ABS	3
7	Winder	STEEL	1
8	Trident Engineering Spur Gearbox 900:1	DONOR COMPONENT	1
9	Gear 3	NYLON	1
10	Custom Torsion Spring	MUSIC WIRE	1
11	Body RHS	ABS	1
12	Canon DN22M-12	Donor Component	1
13	Gear 2	NYLON	1
14	GB - Spur gear 1M 16T 20PA 3FW --- S16A75H50L2.0N	NYLON	1
15	Back Toe	STEEL	2
16	Ankle	ABS	1
17	Foot	ABS	1
18	Front Toe	STEEL	2
19	Gearbox Mount	ABS	1
20	M2 X 6mm Bolt	DONOR COMPONENT	12
21	External Circlip	STEEL	1
22	Gear 4	NYLON	1
23	M2 Nut	DONOR COMPONENT	8
24	Electronics	DONOR COMPONENT	1
25	Battery Case	ABS	1
26	Battery Connector	DONOR COMPONENT	3
27	Crazepony 250mAh 3.7V Lipo Battery	DONOR COMPONENT	3
28	Battery lid	ABS	1
29	Battery Gasket	STEEL	1
30	Body LHS	ABS	1
31	Motor Mount	ABS	1
32	Key	STEEL	1

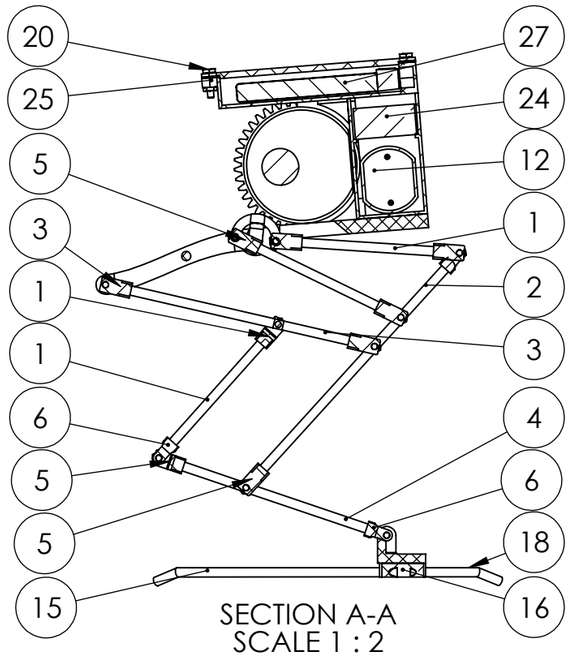

SECTION A-A
SCALE 1 : 2

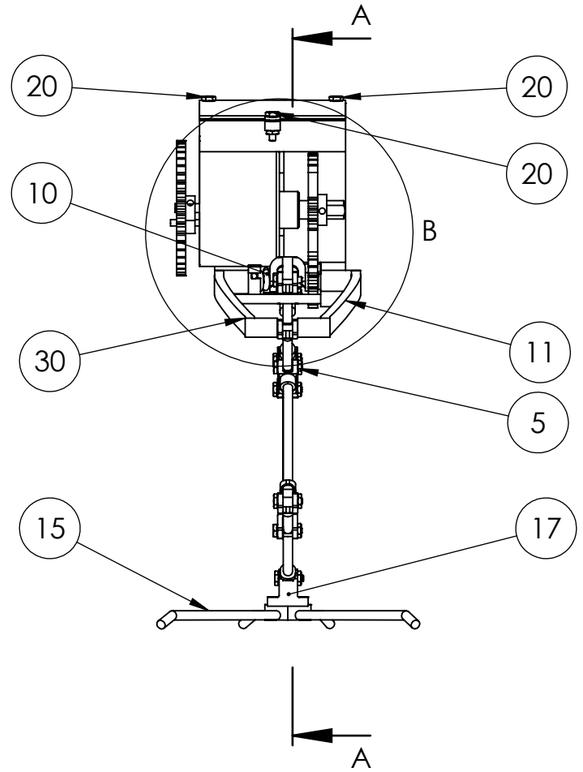

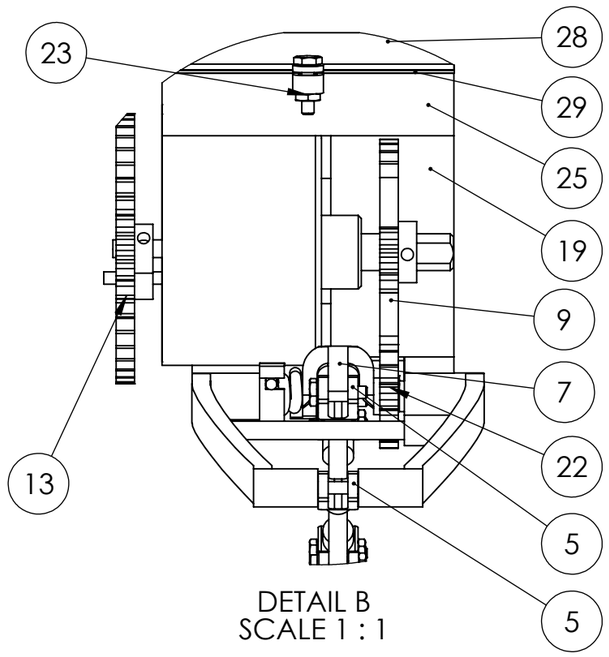

DETAIL B
SCALE 1 : 1

DWG NO. Gizmo Ric Zhang

A3

SCALE:1:2

Total Mass: 194.33 g

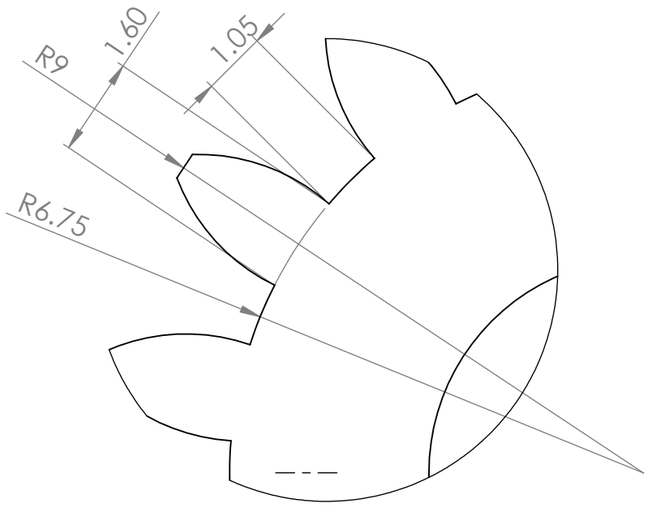

DETAIL A
SCALE 10 : 1

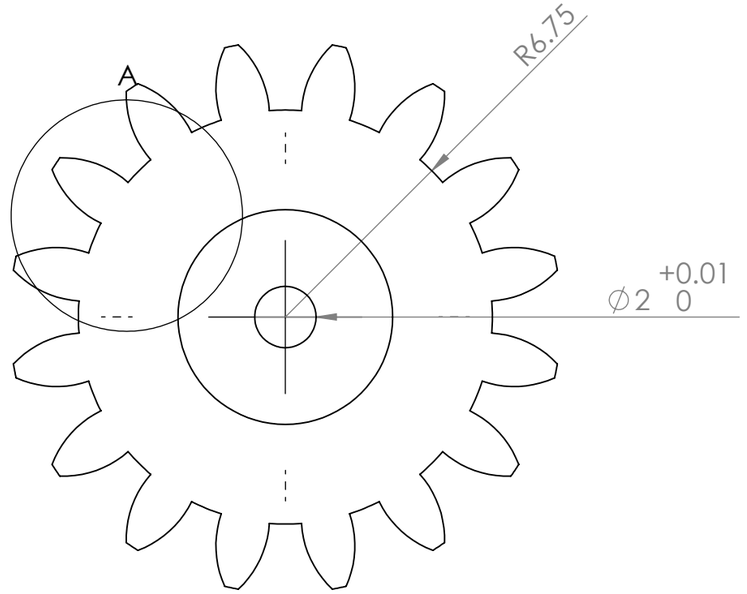

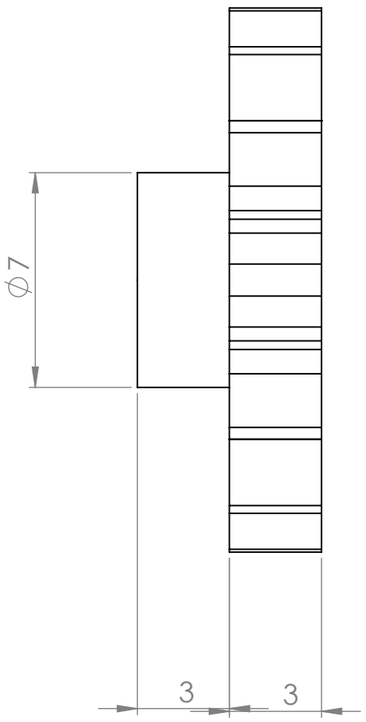

UNLESS OTHERWISE SPECIFIED: DIMENSIONS ARE IN MILLIMETERS SURFACE FINISH: TOLERANCES: LINEAR: ±0.1mm ANGULAR: ±0.15°		FINISH:		DEBURR AND BREAK SHARP EDGES		DO NOT SCALE DRAWING	REVISION
	NAME	SIGNATURE	DATE			TITLE:	
DRAWN							
CHK'D							
APPV'D							
MFG							
Q.A				MATERIAL: NYLON 66		DWG NO. Gear 1	A3
				WEIGHT:		SCALE:5:1	SHEET 1 OF 1

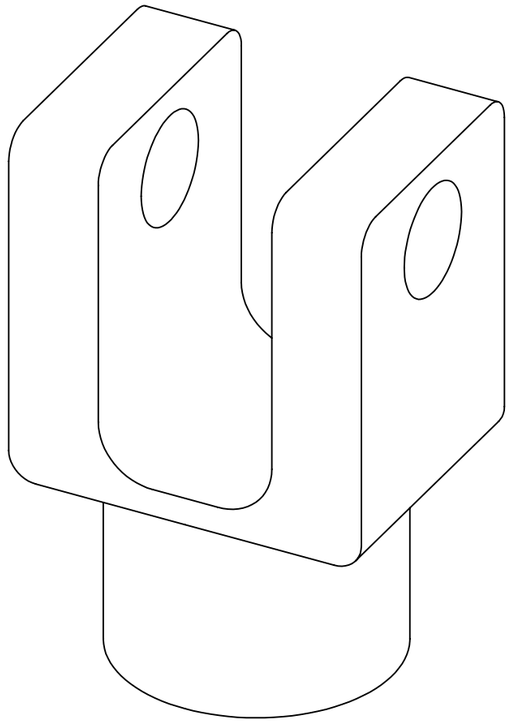

Trimetric View
10:1

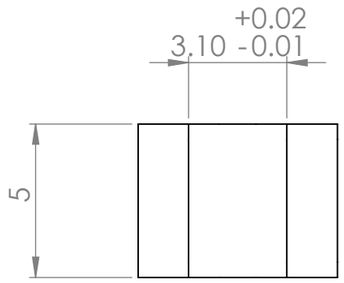

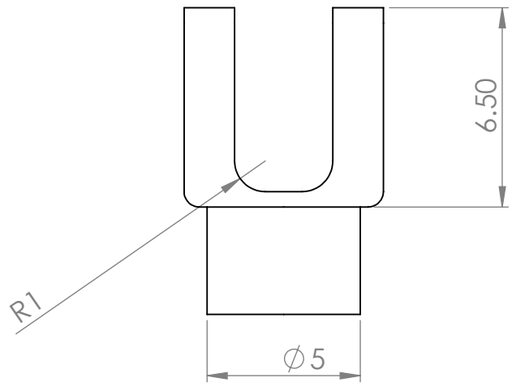

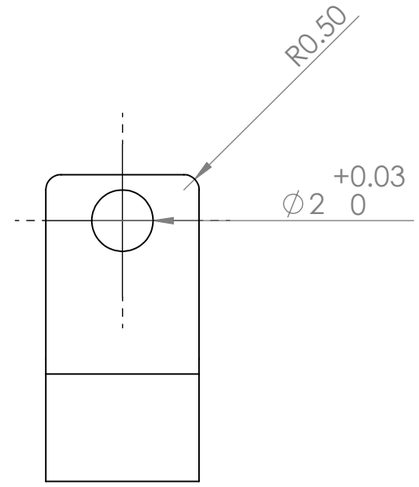

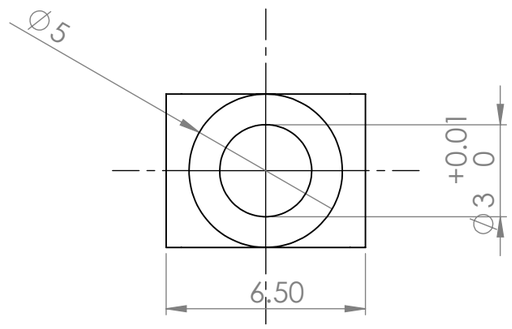

UNLESS OTHERWISE SPECIFIED: DIMENSIONS ARE IN MILLIMETERS SURFACE FINISH: TOLERANCES: LINEAR:±0.1mm ANGULAR:±0.15°		FINISH:		DEBURR AND BREAK SHARP EDGES		DO NOT SCALE DRAWING	REVISION
	NAME	SIGNATURE	DATE			TITLE:	
DRAWN							
CHK'D							
APPV'D							
MFG							
Q.A				MATERIAL: ABS		DWG NO. Female Joint	A3
				WEIGHT:		SCALE:5:1	SHEET 1 OF 1

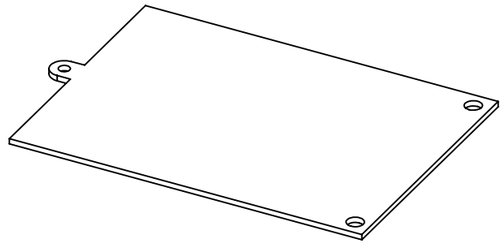

Trimetric View
SCALE 1:1

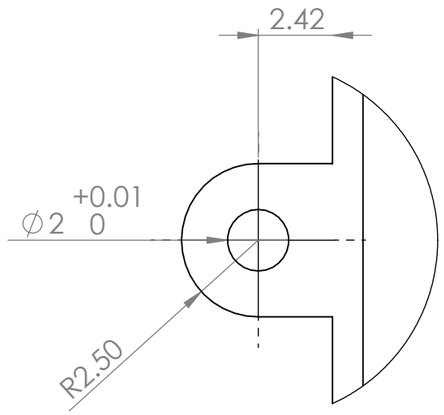

DETAIL A
SCALE 5 : 1

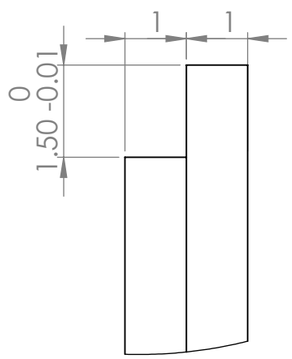

DETAIL B
SCALE 10 : 1

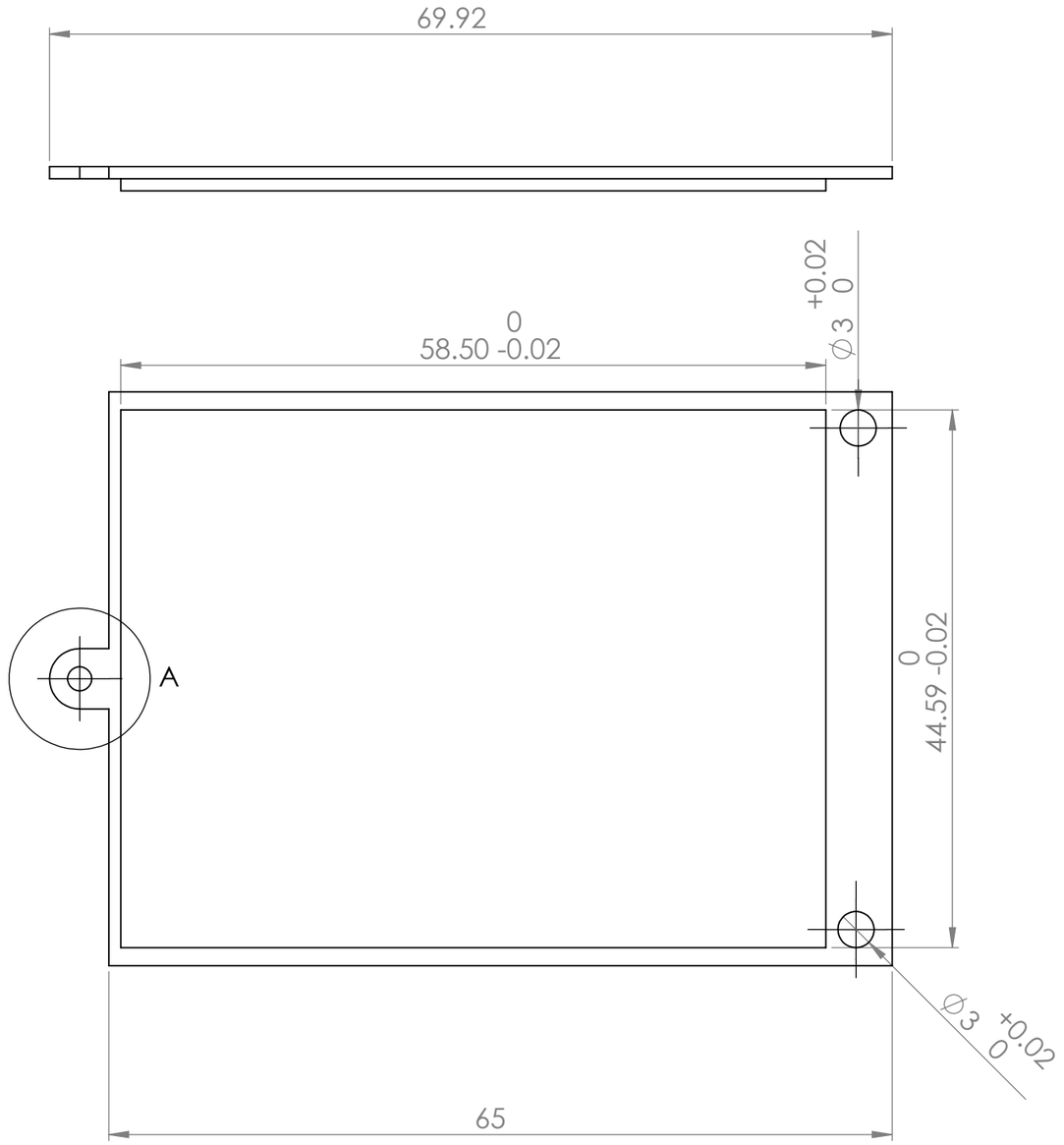

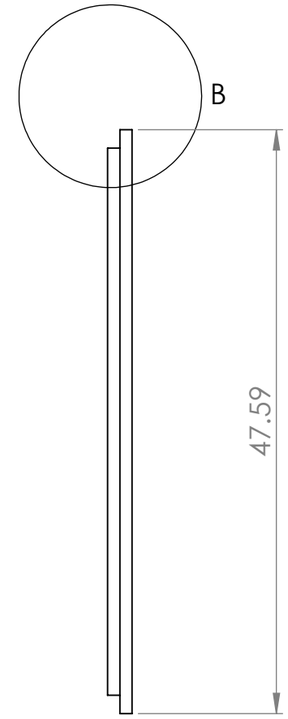

UNLESS OTHERWISE SPECIFIED: DIMENSIONS ARE IN MILLIMETERS SURFACE FINISH: TOLERANCES: LINEAR:±0.1mm ANGULAR:±0.15°		FINISH:		DEBURR AND BREAK SHARP EDGES		DO NOT SCALE DRAWING	REVISION
	NAME	SIGNATURE	DATE				TITLE:
DRAWN							
CHK'D							
APPV'D							
MFG							
Q.A				MATERIAL: ABS		DWG NO. Battery lid	A3
				WEIGHT:		SCALE:2:1	SHEET 1 OF 1